



NIH PUBLIC ACCESS

Author Manuscript

*Chembiochem*. Author manuscript; available in PMC 2014 January 02.

Published in final edited form as:

*Chembiochem*. 2013 January 2; 14(1): 53–57. doi:10.1002/cbic.201200700.

## FRET-CAPTURE: A sensitive method for the detection of dynamic protein interactions

**Dr. Elke Socher and Prof. Barbara Imperiali**

Department of Biology and Department of Chemistry Massachusetts Institute of Technology, Cambridge, MA 02139 (USA)

Barbara Imperiali: imper@mit.edu

### Keywords

fluorescent probe; FRET; solvatochromic dye; protein interaction; protein micro patterning

Identifying and analyzing macromolecular processes such as protein-protein interactions and conformational dynamics are central to chemical biology, biochemistry and medicine. Fluorescence-based sensors are important tools for monitoring these processes. The majority of sensors rely on Förster Resonance Energy Transfer (FRET), which takes advantage of the distance-dependent interaction of two fluorophores to report proximity or/and changes in the fluorophore dipolar interactions. FRET has been extensively used to explore spatiotemporal regulation of various biochemical phenomena.<sup>[1]</sup> The design of FRET-based systems involves strategic positioning of two fluorophores to maximize signal changes enabling the researcher to monitor biological events. Ideally, the FRET-based assays lead to a decrease in the donor emission and an increase of the acceptor emission, allowing FRET processes to be followed by ratiometric measurements. Fluorescent labels can either be fused to two interacting partners to report molecular assembly (intermolecular FRET) or tagged on the same protein to report conformational changes (intramolecular FRET). The integration of fluorescent probes into protein is widespread and often pairs of genetically encoded autofluorescent proteins (FPs) such as the GFP variants CFP/YFP, as donor and acceptor fluorophores, are applied.<sup>[2]</sup> In general, acceptable changes in emission intensities using intramolecular FRET can only be achieved by considerable experimentation with different constructs and often, the signal to background ratios are small due to high background fluorescence. Also, the size (~27 kDa) of the FPs may perturb protein localization and complicate FRET analyses.<sup>[3]</sup>

Alternatively, approaches where synthetic fluorophores are attached to target proteins via self-labeling protein tags such as the SNAP-tag,<sup>[4]</sup> CLIP-tag,<sup>[5]</sup> or Halo-tag<sup>[6]</sup> have proven to be valuable. In this case, the range of synthetic fluorophores that can be recruited is considerable. However, one limitation of these systems is high fluorescence background signal due to the presence of unreacted probes and non-specific binding. Therefore washing steps may be necessary which are not always possible, for example in the real-time measurement of binding events. In this context, useful approaches for reducing background fluorescence have recently been reported.<sup>[7]</sup> In general, FRET-based approaches necessitate considerable inter- or intramolecular distance modulation to observe useful changes in fluorescence. While in some cases the target systems can be engineered to enhance spectral changes, for example in the recent development of a carbonic anhydrase-based FRET

system for sensing benzenesulfonamide,<sup>[8]</sup> there remains the opportunity for new experimental approaches for measuring dynamic protein interactions and conformational changes.

Herein, we present the design, development and validation of an alternative FRET approach that exploits a solvatochromic fluorophore as a FRET donor. This approach addresses some of the shortcomings of traditional FRET-based experiments. In this context we note that methods for investigating the sequence specific recognition of DNA, by exploiting intercalated environment-sensitive fluorophores as FRET donors have been reported.<sup>[9]</sup> Solvatochromic fluorophores like dimethylamino-naphthalimides (DMNs) and dimethylaminophthalimides (DMPs) are sensitive to the local environment and exhibit extremely weak fluorescence in polar protic environments conferring the advantage of low background signals until the occurrence of an event that alters the local environment around the fluorophore. These dyes have been successfully applied in various contexts.<sup>[10]</sup> Recently, we introduced an amino acid based on the solvatochromic fluorophore 4-N,N-dimethylamino-1,8-naphthalimide (4DMN) for sensing binding of M13 (the calmodulin (CaM)-binding peptide)<sup>[11]</sup> to Ca<sup>2+</sup>-activated CaM with a fluorescence increase of up to 100-fold.<sup>[12]</sup> 4DMN has been applied for studying the dynamic interactions of CaM in the apo-state and in the Ca<sup>2+</sup>-bound form.<sup>[13]</sup> Taking a cue from these studies, we envisioned a fluorescence-based approach, termed FRET-CAPTURE, which would combine solvatochromic fluorescence to “turn-on” a donor fluorophore for energy transfer to an acceptor fluorophore thereby exploiting the high apparent Stokes shift of a FRET experiment. A key feature of this method is that in polar protic solvents such as water, the solvatochromic FRET donors in the DMN family are completely non-emissive and therefore background levels of energy transfer are totally absent. In contrast, solvatochromic fluorophores such as BADAN and NBD show background fluorescence in water and when attached to the M13 peptide,<sup>[11]</sup> which would induce an increased FRET signal even in the unbound state. Therefore, the FRET-CAPTURE approach is unique to solvatochromic fluorophores that show a completely non-emissive state. Additionally, in FRET-CAPTURE a conformational change is not necessary and an extra level of specificity is added to the readout since the donor fluorescence is only initiated after target binding. Additionally, while the maximal emission wavelength of 4DMN (~ 505 nm) is in a range where cellular background fluorescence can interfere, the FRET process shifts the emission to more advantageous wavelengths.

Here, we exploit the CaM system for establishing the concepts and potential of the new methodology. Specifically, 4DMN was introduced into the M13 peptide as a fluorescence donor and a second carefully chosen non-solvatochromic fluorophore was attached to the CaM to serve as a FRET acceptor (Fig. 1A) to study the intermolecular modality of FRET-CAPTURE. In general, FRET is dependent on the donor/acceptor distance, the relative orientation of the donor and acceptor transition dipole moments, and the overlap between donor emission and acceptor absorbance. Therefore, several fluorophores, displaying significant spectral overlap with 4DMN, were surveyed at different acceptor positions in the CaM protein to define combinations with optimal FRET efficiency and high fluorescence increases. We also demonstrate an intramolecular FRET-CAPTURE approach using dual labeling of the M13 peptide with both 4DMN and an acceptor fluorophore. The latter approach is illustrated using micropatterning the CaM/M13 peptide interaction on glass surfaces. In this case, an intramolecular FRET-CAPTURE signal is observed even in the absence of any change in the interfluorophore distance.

The M13 peptide was synthesized as described previously,<sup>[12]</sup> and 4DMN was introduced as the Fmoc-protected amino acid (4DMN-A) at position 8 of the native M13 sequence. Fluorescent labeling with the acceptor dye was performed using the CaM cysteine mutants

E11C, M76C and M145C (Figure 1B) enabling selective labeling of the protein with thiol-reactive reagents.

We first explored the influence of the CaM labeling site on the increase of 4DMN fluorescence alone (Fig. S1). Binding of the 4DMN-labeled M13 peptide to the Ca<sup>2+</sup>-activated CaM mutants resulted in varying degrees of fluorescence enhancement. The complexes were analyzed by measuring the ratio of fluorescence intensity at the emission maximum of 4DMN ( $\lambda_{\text{max}} = 505 \text{ nm}$ ) in the Ca<sup>2+</sup>-CaM bound complex to the fluorescence intensity of the apo-state in the presence of the 4DMN-labeled M13 mutant. The 4DMN fluorescence increase achieves the highest value of 180-fold in the M76C CaM mutant complex followed by 98-fold and 43-fold in the E11C and M145C CaM mutant complexes, respectively. Concurrent with the increase in fluorescence intensity was a hypsochromic shift in the emission maximum from 535 nm in the apo-state to 505 nm in the Ca<sup>2+</sup>-bound state. The differences in 4DMN fluorescence resulting from these mutants are attributed to variations in the hydrophobic environment of the fluorophore upon binding.

Next, we investigated the effect of incorporating six potential FRET acceptor fluorophores (Alexa Fluor 555, Alexa Fluor 568, Alexa Fluor 594, Alexa Fluor 633, BODIPY®-TMR and BODIPY®-577) into each of the three cysteine mutants of CaM. Representative FRET-CAPTURE data for the E11C CaM mutant, which is labeled using Alexa Fluor® dyes with varying excitation wavelengths is shown in Fig. 2 (See SI for the complete data set). Fluorescence spectra were recorded upon donor excitation for (1) the acceptor-only labeled CaM in the apo-state; (2) CaM in the Ca<sup>2+</sup>-bound state; (3) CaM in the presence of 4DMN-labeled M13 peptide in the apo-state; (4) CaM in the Ca<sup>2+</sup>-bound state with the 4-DMN-labeled M13 (Fig. 2). The acceptor dyes showing the largest spectral overlap are Alexa Fluor 555 (Fig. 2A) and BODIPY®-TMR (Fig. S2E). However, the fluorescence response of the Alexa Fluor 555-labeled calmodulin mutant alone was negligible after excitation of the donor absorbance in the apo- and in the Ca<sup>2+</sup>-bound-state. Importantly, in the absence of Ca<sup>2+</sup>, the dual labeled system showed a similar negligible fluorescence emission upon excitation at 395 nm. However, formation of the structured Ca<sup>2+</sup>-bound complex resulted in a fluorescence increase due to FRET from the bound 4DMN and was accompanied by a shift of the fluorescence emission maximum from 505 nm to 570 nm compared to the 4DMN only labeled system. The FRET signal shows robust 23-fold fluorescence increase. Also illustrated (Fig. 2) are fluorescence studies with Alexa Fluor 594 and Alexa Fluor 633-modified E11C CaM. Upon addition of the 4DMN-M13 peptide, the Alexa 594 construct showed a modest 5.5-fold increase in fluorescence at 611 nm due to FRET-CAPTURE. In addition, the direct fluorescence emission from 4DMN increased 113.7-fold. There was no acceptor fluorescence increase for Alexa Fluor 633, which is the dye with the smallest spectral overlap with CaM-bound 4DMN. The main emission signal that is observed results from the donor fluorescence and the acceptor signal is about 3.4-fold smaller.

We also explored the fluorescence response of the M76C and M145C acceptor-labeled calmodulin mutants (Fig. S3 and S4). The donor and FRET-fluorescence increases for the three mutants with Alexa Fluors 555, 594 and 633 are summarized in Fig. 3. The overall observation was that the 4DMN/Alexa Fluor 555 pair demonstrated the highest FRET fluorescence increase (23.4–25.1-fold). Interestingly the fluorescence increases did not vary greatly amongst the three mutants, due to the fact that the interfluorophore distance was relatively small and in a range where FRET efficiency would be insensitive to distance ( $R_0$ , for estimation of  $R_0$  see SI). We note that the NMR structure of CaM bound to M13 (PDB: 2BBM) shows that the C- site of M145, M76, and E11 is approximately 9 Å, 21 Å, 12 Å away from the 8 position of the M13 peptide.

A comparison of the fluorescence background intensity of the acceptor only-labeled CaM reveals no change in emission with addition of  $\text{Ca}^{2+}$ . For detection of protein interactions in complex environments it would be reasonable to subtract the background (FBG- $\text{Ca}^{2+}$  and FBG-EGTA) first before dividing the intensity of the bound-state by the intensity of the apo-state. The resulting background-corrected FRET fluorescence increase  $[(\text{FFRET} - \text{FBG})\text{Ca}^{2+}/(\text{FFRET} - \text{FBG})\text{EGTA}]$  is shown in Figs. 3B,D,F (dark grey bars). With this analysis an average fluorescence increase of ~11.3-fold for Alexa Fluor 594 acceptor dyes would be observed, while no significant change in the FRET fluorescence increase would be observed for the Alexa Fluor 555 since the background fluorescence of Alexa Fluor 555 is low enough that the signal does not interfere with the FRET measurement. Background correction of the Alexa Fluor 633 signal increases the average FRET fluorescence enhancement from 1.7-fold to 3.5-fold. This analysis reveals opportunities for applications that involve multiplexing since the FRET-CAPTURE from bound 4DMN to spectrally distinguishable FRET acceptors could potentially be observed.

We also investigated intramolecular FRET-CAPTURE by observing the effect of dual labeling of the M13 peptide. In this case, the environment-sensitive donor dye 4DMN was retained at position 8 (M13 peptide) and the acceptor fluorophore was incorporated at the N-terminus of the peptide by using cysteine modification chemistry. The fluorescence spectrum of the donor-only labeled M13 peptide, with an additional N-terminal cysteine, revealed a 41-fold fluorescence change from the unbound to the protein bound state (Fig. S5). We then evaluated the three acceptor dyes Alexa Fluor 555, Alexa Fluor 568, and Alexa Fluor 594 that demonstrated good fluorescence increases in the intermolecular FRET-CAPTURE experiments and also gave high labeling efficiencies. The 4DMN/Alexa 555 pair demonstrated the best performance (Fig. 4A and S6). The fluorescence signal of the unbound 4DMN/Alexa 555-labeled M13 peptide showed a minimal background acceptor emission spectrum in the presence of CaM. After  $\text{Ca}^{2+}$  addition, a significant 4.9-fold increase in the acceptor fluorescence was observed.

A major source of high background in complex biological environments is due to non-specific binding. To demonstrate the high specificity of the FRET-CAPTURE signal, the 4DMN/Alexa 555-labeled M13 peptide was added to HeLa cell lysates and fluorescence was measured in the presence and absence of  $\text{Ca}^{2+}$  (Fig. 4B). In the absence of  $\text{Ca}^{2+}$ , no significant background fluorescence compared to a simple TBS buffered solution was observed (Fig S8A). In the presence of  $\text{Ca}^{2+}$ , the dual labeled peptide signaled a low level of endogenous CaM with a FRET-CAPTURE signal increase of 1.6-fold (60%), which was stable over time and reversible in the presence of added EGTA (Fig. S8B). Addition of recombinant CaM increased the FRET-CAPTURE signal increase up to 3.1-fold.

The response of the 4DMN/Alexa Fluor 555 pair made this an optimal system for investigating whether FRET-CAPTURE was suitable for monitoring binding events on modified glass surfaces. Proteins and peptides are commonly printed on modified glass surfaces for applications in biosensing, bioanalysis, as well as small molecule screening.<sup>[14]</sup> Creating a FRET-CAPTURE pattern with the CaM/M13 peptide construct demonstrates the sensitivity of the system to fluoresce in a well-defined monolayer bound to a surface. Biotin surface patterns were obtained by using amino-functionalized glass surfaces, micro-patterned with PDMS-stamps inked in NHS-PEG-biotin, to define binding sites. The remaining functional groups on the surface were blocked using NHS-PEG<sub>8</sub>. Streptavidin was attached to the biotin-patterned substrates followed by biotinylated CaM (E11C mutant) to create a CaM pattern (Fig. 4C). In the last step, the 4DMN/Alexa Fluor 555 labeled M13 peptide was brought in contact with CaM in a buffer containing  $\text{Ca}^{2+}$  and a FRET-CAPTURE pattern was monitored using confocal microscopy. The imaging revealed both the 4DMN (green) and the FRET- (red) emission with a strong fluorescence contrast

between the background and the stamped regions (Fig 4D). In the negative control the 4DMN/Alexa Fluor 555 labeled M13 peptide was added to the CaM pattern in a buffer without Ca<sup>2+</sup> (Fig. 4E). While background fluorescence was visible, the unbound state could be clearly discriminated from the bound state. In a further control, the addition of CaM was omitted, demonstrating that the fluorescence signal is attributed only to the specific binding (Fig. S9C). A pattern produced with the 4DMN-only labeled M13 peptide (Fig. S9D) revealed only sharp features in the emission range of the donor.

In summary, we have presented the principles of inter- and intramolecular FRET-CAPTURE to signal protein interactions and conformational changes by exploiting the unique donor fluorescence of a bound solvatochromic dye (4DMN) coupled with selected acceptor fluorophores, which afford an advantageous bathochromic shift of the emission wavelength. The method has been demonstrated to be useful in simple buffer systems, unfractionated cell lysates and on micro-patterned glass surfaces. The detected 20–30-fold FRET-fluorescence increases achieved by applying the 4DMN/Alexa 555 pair compares favourably with reported FRET-enhancements for protein sensing. The background fluorescence, depending on the FRET acceptor is either negligible or very low, and no washing steps are necessary to remove unbound or non-specific bound probes. A unique feature of the presented FRET-CAPTURE method is the additional level of signal selectivity since the FRET signal is only turned on when the donor is specifically bound to the protein of interest, eliminating false positive results. The probes provide two readout modes after donor excitation to detect protein-interactions: I) Donor emission at 505 nm and II) FRET-CAPTURE emission depending on the acceptor from 570 – 644 nm, revealing a high apparent Stokes shift of more than 170 nm. The ability to apply acceptor fluorophores with unique emission properties further suggests that the method could be expanded to include the simultaneous application of two suitable FRET-pairs, which would enable multiplexing.

## Supplementary Material

Refer to Web version on PubMed Central for supplementary material.

## Acknowledgments

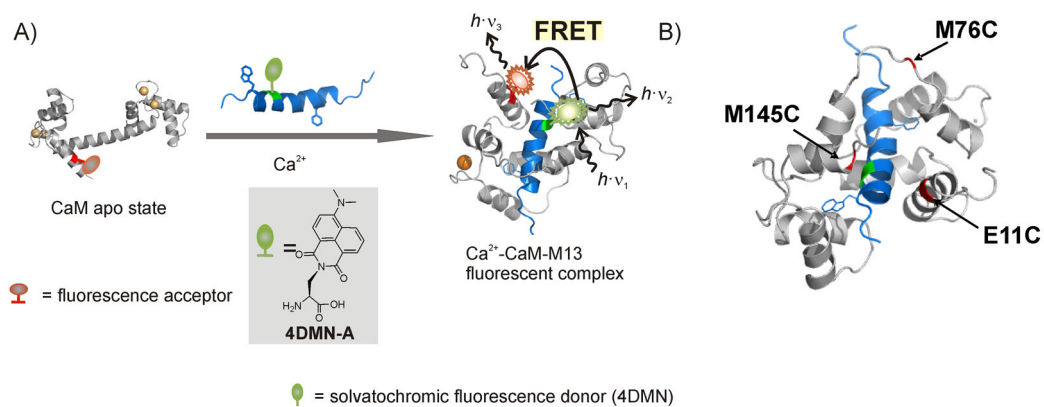
This work was supported by the National Institutes of Health (NIH) grant number (R01 EB010246). E. Socher was supported by a postdoctoral fellowship from DFG (Deutsche Forschungsgemeinschaft, SO 1100/1-1).

The authors thank Mr. Ben Stinson for technical assistance in the early stage of these studies.

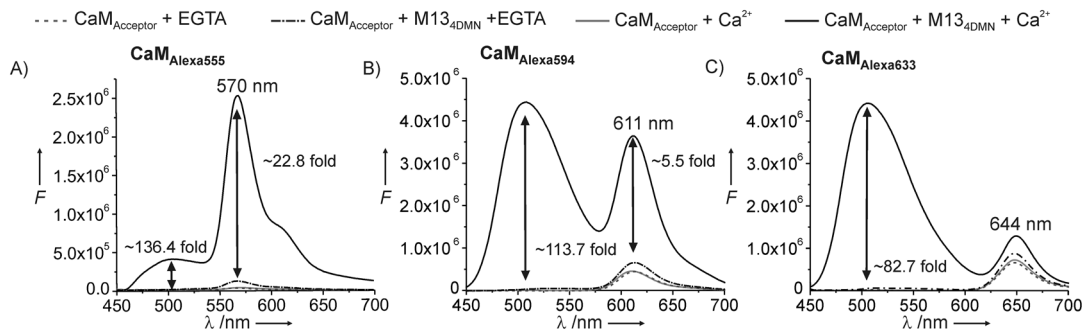
## References

1. a) Padilla-Parra S, Tramier M. *Bioessays*. 2012; 34:369–376. [PubMed: 22415767] Miyawaki A. *Annu Rev Biochem*. 2011; 80:357–373. [PubMed: 21529159] b) Uphoff S, Holden SJ, Le Reste L, Periz J, van de Linde S, Heilemann M, Kapanidis AN. *Nat Methods*. 2010; 7:831–836. [PubMed: 20818380] c) Roy R, Hohng S, Ha T. *Nat Methods*. 2008; 5:507–516. [PubMed: 18511918]
2. a) Chalfie M, Tu Y, Euskirchen G, Ward WW, Prasher DC. *Science*. 1994; 263:802–805. [PubMed: 8303295] b) Miyawaki A, Llopis J, Heim R, McCaffery JM, Adams JA, Ikura M, Tsien RY. *Nature*. 1997; 388:882–887. [PubMed: 9278050] c) Zhao Y, Araki S, Wu J, Teramoto T, Chang YF, Nakano M, Abdelfattah AS, Fujiwara M, Ishihara T, Nagai T, Campbell RE. *Science*. 2011; 333:1888–1891. [PubMed: 21903779] d) Miyawaki A. *Dev Cell*. 2003; 4:295–305. [PubMed: 12636912]
3. Piljic A, de Diego I, Wilmanns M, Schultz C. *ACS Chem Biol*. 2011; 6:685–691. [PubMed: 21506563]
4. Keppler A, Gendrezig S, Gronemeyer T, Pick H, Vogel H, Johnsson K. *Nat Biotechnol*. 2003; 21:86–89. [PubMed: 12469133]

5. Gautier A, Juillerat A, Heinis C, Correa IR Jr, Kindermann M, Beaufile F, Johnsson K. *Chem Biol*. 2008; 15:128–136. [PubMed: 18291317]
6. Los GV, Encell LP, McDougall MG, Hartzell DD, Karassina N, Zimprich C, Wood MG, Learish R, Ohana RF, Urh M, Simpson D, Mendez J, Zimmerman K, Otto P, Vidugiris G, Zhu J, Darzins A, Klaubert DH, Bulleit RF, Wood KV. *ACS Chem Biol*. 2008; 3:373–382. [PubMed: 18533659]
7. a) Maurel D, Banala S, Laroche T, Johnsson K. *ACS Chem Biol*. 2010; 5:507–516. [PubMed: 20218675] b) Sun X, Zhang A, Baker B, Sun L, Howard A, Buswell J, Maurel D, Masharina A, Johnsson K, Noren CJ, Xu MQ, Correa IR Jr. *Chembiochem*. 2011; 12:2217–2226. [PubMed: 21793150] c) Hori Y, Nakaki K, Sato M, Mizukami S, Kikuchi K. *Angew Chem, Int Ed*. 2012; 51:5611–5614.
8. a) Brun MA, Tan KT, Nakata E, Hinner MJ, Johnsson K. *J Am Chem Soc*. 2009; 131:5873–5884. [PubMed: 19348459] b) Brun MA, Griss R, Reymond L, Tan KT, Piguet J, Peters RJ, Vogel H, Johnsson K. *J Am Chem Soc*. 2011; 133:16235–16242. [PubMed: 21879732]
9. a) Socher E, Bethge L, Knoll A, Jungnick N, Herrmann A, Seitz O. *Angew Chem, Int Ed*. 2008; 47:9555–9559. b) Vazquez O, Sanchez MI, Mascarenas JL, Vazquez ME. *Chem Commun (Camb)*. 2010; 46:5518–5520. [PubMed: 20458409]
10. a) Vazquez ME, Rothman DM, Imperiali B. *Org Biomol Chem*. 2004; 2:1965–1966. [PubMed: 15254619] b) Vazquez ME, Blanco JB, Imperiali B. *J Am Chem Soc*. 2005; 127:1300–1306. [PubMed: 15669870] c) Sainlos M, Iskenderian WS, Imperiali B. *J Am Chem Soc*. 2009; 131:6680–6682. [PubMed: 19388649] d) Iskenderian-Epps WS, Imperiali B. *Chembiochem*. 2010; 11:1979–1984. [PubMed: 20715264] e) Vazquez ME, Blanco JB, Salvadori S, Trapella C, Argazzi R, Bryant SD, Jinsmaa Y, Lazarus LH, Negri L, Giannini E, Lattanzi R, Colucci M, Balboni G. *J Med Chem*. 2006; 49:3653–3658. [PubMed: 16759107] f) Venkatraman P, Nguyen TT, Sainlos M, Bilsel O, Chitta S, Imperiali B, Stern LJ. *Nat Chem Biol*. 2007; 3:222–228. [PubMed: 17351628] g) Goguen BN, Loving GS, Imperiali B. *Bioorg Med Chem Lett*. 2011; 21:5058–5061. [PubMed: 21549598] h) Fuller AA, Seidl FJ, Bruno PA, Plescia MA, Palla KS. *Biopolymers*. 2011; 96:627–638. [PubMed: 22180910] i) Yang M, Song Y, Zhang M, Lin S, Hoa Z, Liang Y, Zhang D, Chen PR. *Angew Chem, Int Ed*. 2012; 51:7674–7679.
11. a) Ikura M, Clore GM, Gronenborn AM, Zhu G, Klee CB, Bax A. *Science*. 1992; 256:632–638. [PubMed: 1585175] b) Porumb T, Yau P, Harvey TS, Ikura M. *Protein Eng*. 1994; 7:109–115. [PubMed: 8140087]
12. Loving G, Imperiali B. *J Am Chem Soc*. 2008; 130:13630–13638. [PubMed: 18808123]
13. Loving G, Imperiali B. *Bioconjug Chem*. 2009; 20:2133–2141. [PubMed: 19821578]
14. Blawas AS, Reichert WM. *Biomaterials*. 1998; 19:595–609. [PubMed: 9663732]

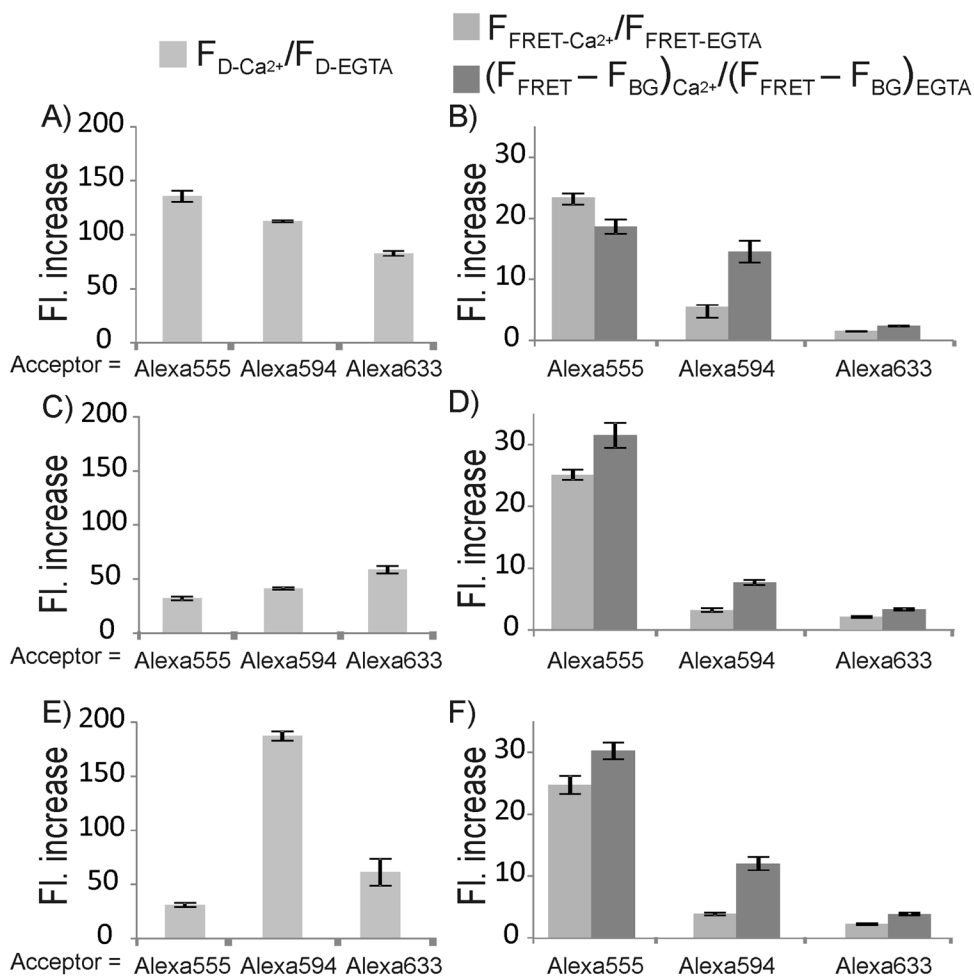
**Figure 1.**

A) FRET-CAPTURE for sensing the  $\text{Ca}^{2+}$  induced interaction between CaM and the M13 peptide. The M13 peptide mutant (blue) contains the solvatochromic fluorophore 4DMN as an amino acid building block (green) that signals binding of the M13 peptide to the  $\text{Ca}^{2+}$  activated CaM (grey) to an acceptor dye (red) attached to CaM by FRET. B) The positions of the acceptor in the three different cysteine mutants are marked in red in the NMR structure of the  $\text{Ca}^{2+}$ -CaM-M13 peptide complex (PDB: 2BBM).

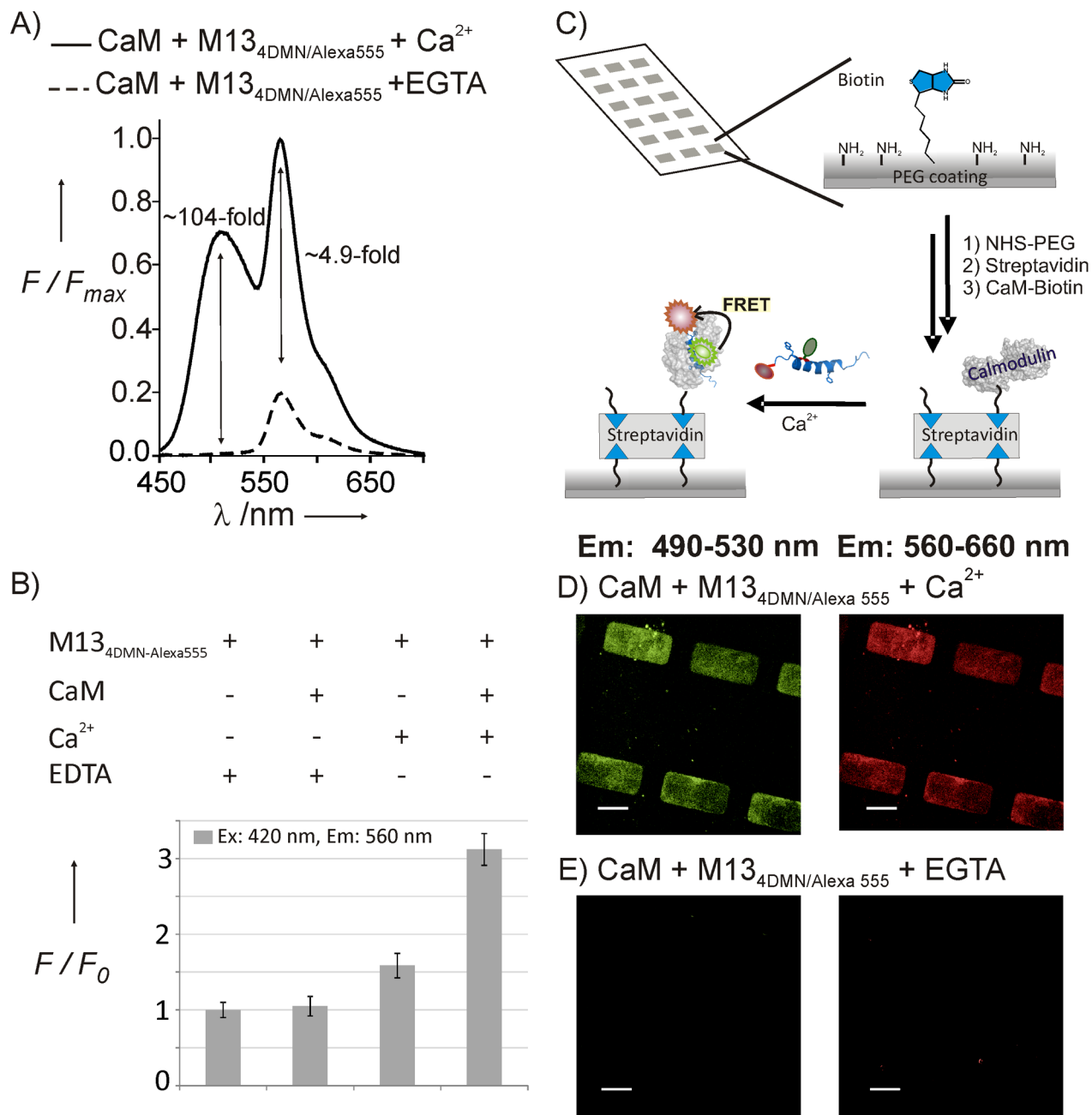
**Figure 2.**

Fluorescence measurements after 4DMN excitation in the acceptor only labeled E11C CaM mutant (black) and in the dual-labeled E11C CaM<sub>Acceptor</sub> mutant/M13<sub>4DMN</sub> peptide construct (red) in the absence (dashed line) and presence (solid line) of Ca<sup>2+</sup>. Acceptor = A) Alexa555, B) Alexa594, and C) Alexa633. Conditions: 400 nM CaM, 400 nM M13<sub>4DMN</sub>, 200  $\mu$ M CaCl<sub>2</sub>, 40  $\mu$ M EGTA in TBS, 25°C, pH = 7.4,  $E_{Ex}^*$  = A) 395 nm; B) + C) 435 nm; slit<sub>Ex</sub> 10 nm, slit<sub>Em</sub> 5 nm. (\*Different excitation wavelengths are used according to minimize donor-independent fluorescence.)





**Figure 3.** Signal to background ratios: Right panels demonstrate donor fluorescence increases and left panels show FRET fluorescence increases. A) and B) E11C CaM mutant/M13 peptide; C) and D) M76C CaM mutant/M13 peptide and E) and F) M145C CaM mutant/M13 peptide.  $F_D$  is the donor fluorescence at 505 nm,  $F_{FRET}$  is the FRET fluorescence, and  $F_{BG}$  is the fluorescence of only acceptor labeled CaM (Background).  $F_{FRET}$  and  $F_{BG}$  are measured at the acceptor emission maximum. (Conditions: see Figure 2).

**Figure 4.**

Measurement of intramolecular FRET-CAPTURE using the 4DMN/Alexa555-labeled M13 peptide A) in the presence of the E11C CaM mutant in the apo state (dashed lines) and in the Ca<sup>2+</sup>-state (solid line) after excitation of the 4DMN ( $\lambda_{EX} = 435$  nm). (Conditions: 800 nM CaM E11C, 600 nM M13 in TBS, see Figure 2) and B) in HeLa cell lysates in the presence and absence Ca<sup>2+</sup> before and after adding recombinant CaM. (Conditions: 200 nM M13, 800 nM CaM when added.) C) Scheme of creating a CaM/M13<sub>4DMN/Alexa555</sub> peptide micro-pattern which shows fluorescence in the presence of Ca<sup>2+</sup> for both, donor and acceptor fluorophore. D–E) Confocal laser scanning microscopy images of the CaM/M13 peptide pattern on glass. Dual-labeled Alexa/4DMN-M13 peptide was added to D) Ca<sup>2+</sup>-activated

CaM, or to E) CaM in the apo-state. Images were taken with a confocal laser scanning microscope at rt and  $\lambda_{\text{ex}} = 458 \text{ nm}$ . White bars:  $30 \mu\text{m}$ .